Critical roles of $G_{i/o}$ proteins and phospholipase C-δ1 in the activation of receptor-operated TRPC4 channels

Dhananjay P. Thakur[a,b], Jin-bin Tian[a], Jaepyo Jeon[a], Jian Xiong[a,b], Yu Huang[a,b], Veit Flockerzi[c], and Michael X. Zhu[a,b,1]

[a]Department of Integrative Biology and Pharmacology, The University of Texas Health Science Center at Houston, Houston, TX 77030; [b]Graduate Studies in Cell and Regulatory Biology, The University of Texas Health Science Center at Houston, Houston, TX 77030; and [c]Experimental and Clinical Pharmacology and Toxicology, Saarland University, 66421 Homburg, Germany

Edited by Ramon Latorre, Centro Interdisciplinario de Neurociencias, Universidad de Valparaíso, Valparaíso, Chile, and approved December 18, 2015 (received for review November 13, 2015)

Transient Receptor Potential Canonical (TRPC) proteins form nonselective cation channels commonly known to be activated downstream from receptors that signal through phospholipase C (PLC). Although TRPC3/C6/C7 can be directly activated by diacylglycerols produced by PLC breakdown of phosphatidylinositol 4,5-bisphosphate (PIP_2), the mechanism by which the PLC pathway activates TRPC4/C5 remains unclear. We show here that TRPC4 activation requires coincident stimulation of $G_{i/o}$ subgroup of G proteins and PLCδ, with a preference for PLCδ1 over PLCδ3, but not necessarily the PLCβ pathway commonly thought to be involved in receptor-operated TRPC activation. In HEK293 cells coexpressing TRPC4 and $G_{i/o}$-coupled μ opioid receptor, μ agonist elicited currents biphasically, with an initial slow phase preceding a rapidly developing phase. The currents were dependent on intracellular Ca^{2+} and PIP_2. Reducing PIP_2 through phosphatases abolished the biphasic kinetics and increased the probability of channel activation by weak $G_{i/o}$ stimulation. In both HEK293 cells heterologously expressing TRPC4 and renal carcinoma-derived A-498 cells endogenously expressing TRPC4, channel activation was inhibited by knocking down PLCδ1 levels and almost completely eliminated by a dominant-negative PLCδ1 mutant and a constitutively active RhoA mutant. Conversely, the slow phase of $G_{i/o}$-mediated TRPC4 activation was diminished by inhibiting RhoA or enhancing PLCδ function. Our data reveal an integrative mechanism of TRPC4 on detection of coincident $G_{i/o}$, Ca^{2+}, and PLC signaling, which is further modulated by the small GTPase RhoA. This mechanism is not shared with the closely related TRPC5, implicating unique roles of TRPC4 in signal integration in brain and other systems.

TRP channels | G proteins | pertussis toxin | phospholipase C | calcium

Of the Transient Receptor Potential (TRP) superfamily, the Canonical TRPs (TRPC1–7) are the most homologous to the prototypical *Drosophila* TRP and are believed to be activated downstream of phospholipase C (PLC) (1). In both heterologous and native systems, stimulating PLCβ via the $G_{q/11}$ subgroup of G proteins is commonly used to activate TRPC channels. Recent studies, however, also suggest a role for $G_{i/o}$ subgroup of G proteins in the activation of TRPC4/C5 (2–4).

TRPC4 is implicated in the regulation of microvascular permeability (5), renal cancer proliferation (6, 7), neurotransmitter release (8), intestinal contraction and motility (9), neurite extension (10), epileptiform burst firing, and seizure-induced neurodegeneration (11). The channel mediates Na^+ and Ca^{2+} influx, causing membrane depolarization and intracellular Ca^{2+} concentration ($[Ca^{2+}]_i$) elevation, which in turn alter cell function (12). Although advances have been made in demonstrating TRPC4 channel activation under $G_{i/o}$ and/or PLC stimulation, as well as its dependence on $[Ca^{2+}]_i$, a precise description of signaling events underlying the mechanism of TRPC4 activation remains elusive.

Here, we distinguished the contributions of $G_{q/11}$ and $G_{i/o}$ pathways to TRPC4 activation and uncovered a strict codependence on $G_{i/o}$ and PLC pathways. We focused on constituents of PLC signaling that cooperated with $G_{i/o}$ to activate TRPC4 and unexpectedly discovered a necessity of PLCδ1, a PLC isoform co-regulated by Ca^{2+} and phosphatidylinositol 4,5-bisphosphate (PIP_2).

Results

TRPC4 Activation Requires Coincident $G_{i/o}$ Stimulation and PLC Activity. When overexpressed in HEK293 cells, both $G_{q/11}$- and $G_{i/o}$-coupled muscarinic receptors (MRs) have been used to trigger TRPC4 currents (4). However, despite the presence of endogenous $G_{q/11}$-coupled MRs (*SI Appendix*, Fig. S1), muscarinic agonist carbachol (CCh, 10–100 μM) elicited very small (or no) currents in cells that stably coexpressed μ opioid receptor (μOR) (13) with either TRPC4β or TRPC4α (Fig. 1*A* and *SI Appendix*, Fig. S2 *A* and *B*). Subsequent addition of μ agonist DAMGO (1 μM) caused robust currents, with current–voltage (I–V) relationships typical of TRPC4/C5, such as a negative slope between 10 and 40 mV and outward rectification at more positive potentials (2–4, 14–16). The near-linear I–V relation at negative potentials indicates very strong channel activation (14, 15). Consistent with μOR being $G_{i/o}$-coupled, the currents were abolished by treatment with pertussis toxin (PTX) (*SI Appendix*, Fig. S2 *A*, *B*, and *E*). Interestingly, although CCh did not evoke TRPC4 currents via endogenous receptors, overexpressing $G_{q/11}$-coupled M1, M3, or M5 MRs with TRPC4 allowed CCh to induce such currents, which to our surprise were also blocked by PTX (*SI Appendix*, Figs. S2 *C–E* and S3). Thus, all overexpressed MRs may activate TRPC4 via $G_{i/o}$ proteins. By contrast, TRPC5 activation was only partially blocked by PTX when stimulated via either endogenous or overexpressed M3R (*SI Appendix*, Fig. S4 *A* and *B*). Therefore, TRPC4, but not TRPC5, exhibits an absolute dependence on $G_{i/o}$ proteins.

We then asked if $G_{i/o}$ stimulation alone is sufficient to activate TRPC4. With $[Ca^{2+}]_i$ weakly buffered by 0.2 mM EGTA in the recording pipette, DAMGO (1 μM) elicited currents in the majority

Significance

Transient Receptor Potential Canonical 4 (TRPC4) forms nonselective cation channels implicated in multiple functions in the brain, heart, vasculature, and gastrointestinal tract. However, mechanisms that govern TRPC4 channel activation remain mysterious, severely hampering their functional elucidation under physiological and pathological conditions. Uniquely, TRPC4 is activated following ligand stimulation of G protein-coupled receptors that function through either $G_{q/11}$ or $G_{i/o}$ subgroups of G proteins. However, to what extent and how these two metabotropic pathways interact to regulate TRPC4 is unclear. Our study demonstrates the critical involvement of $G_{i/o}$ signaling and phospholipase C activity in TRPC4 activation, providing detailed dissection of signaling steps of the phospholipase C pathway that contribute to channel gating. The mechanistic insights revealed should greatly facilitate evaluation and understanding of the physiological and pathological functions of these channels.

Author contributions: D.P.T. and M.X.Z. designed research; D.P.T., J.-b.T., J.J., J.X., and Y.H. performed research; V.F. contributed new reagents/analytic tools; D.P.T., J.-b.T., and M.X.Z. analyzed data; and D.P.T., V.F., and M.X.Z. wrote the paper.

The authors declare no conflict of interest.

This article is a PNAS Direct Submission.

[1]To whom correspondence should be addressed. Email: Michael.x.zhu@uth.tmc.edu.

This article contains supporting information online at www.pnas.org/lookup/suppl/doi:10.1073/pnas.1522294113/-/DCSupplemental.

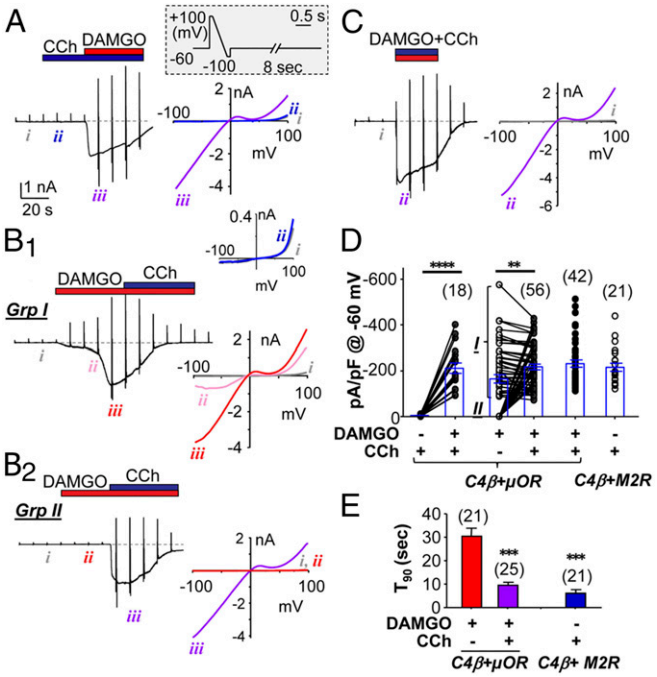

Fig. 1. Differential effects of $G_{q/11}$ and $G_{i/o}$ stimulation on TRPC4 activation. (*A–C*) Representative whole-cell currents of HEK293 cells co-expressing μOR and TRPC4β (μOR/C4β cells). The pipette solution contained 0.2 mM EGTA and no Ca^{2+}. Currents were continuously recorded at –60 mV; voltage ramps from +100 to –100 mV (each held for 100 ms) within 500 ms were applied every 10 s (shaded box), which gave the vertical lines in current traces and are expanded to show the I–V relationship for selected time points (*Right* sides). Dashed lines indicate zero current. CCh (10 μM) and/or DAMGO (1 μM) was added as indicated. The I–V curves before and after CCh application in *A* are expanded to show the very weak effect of CCh on TRPC4 activation. For DAMGO stimulation alone (*B*), cells were divided into group I (Grp I, B_1) and group II (Grp II, B_2) as DAMGO-responsive and irresponsive, respectively. Co-application of DAMGO and CCh evoked currents in all cells (*C*). (*D*) Peak current density at –60 mV induced by DAMGO and/or CCh for individual cells. Blue boxes and bars show means ± SEM. Note the clear segregation between Grp I and Grp II cells in response to DAMGO alone was abolished by CCh. (*E*) Summary of T_{90} at –60 mV for cells stimulated with DAMGO and/or CCh. $^{**}P < 0.01$, $^{***}P < 0.001$, $^{****}P < 0.0001$ by *t* test. Cell numbers are shown in parentheses.

(~71%, designated as group 1 or Grp I) of TRPC4β/μOR-expressing cells (Fig. 1 B_1 and *D*). This proportion was increased to ~100%, with EGTA decreased to 0.05 mM (*SI Appendix*, Fig. S5 *A* and *B*). Subsequent addition of CCh (10 or 30 μM) did not further enhance the currents (Fig. 1 B_1 and *D* and *SI Appendix*, Fig. S5*A*). It is unlikely that DAMGO caused TRPC4 activation via stimulating PLCβ, as DAMGO induced Ca^{2+} transients only in ~2% of HEK293 cells stably expressing μOR (*SI Appendix*, Fig. S1). However, the DAMGO-evoked TRPC4β current was inhibited by intracellular dialysis of the PLC inhibitor U73122 (*SI Appendix*, Fig. S5*C*), suggesting that PLC activity is required, although it may not necessarily be PLCβ. On the other hand, CCh enhanced the probability of DAMGO to activate TRPC4β. With 0.2 mM EGTA, all cells previously exposed to CCh responded to DAMGO with robust currents (Fig. 1 *A* and *D*); the DAMGO-irresponsive cells (Grp II) responded to subsequent CCh application with robust currents (Fig. 1 B_2 and *D*); all cells responded to co-application of DAMGO and CCh with large currents (Fig. 1 *C* and *D*). Thus, the $G_{q/11}$–PLCβ pathway facilitated $G_{i/o}$ activation of TRPC4.

Noticeably, despite the similar maximal (peak) amplitudes as that evoked by DAMGO + CCh (Fig. 1*D*), the currents evoked by DAMGO alone developed very slowly, exhibiting biphasic kinetics—an initial slow phase followed by a fast-rising one (Fig. 1B_1)—similar to that reported previously for TRPC5 (15). Co-application of CCh eliminated the slow phase (Fig. 1 *A*, B_2, and *C*). Quantification of time to 90% peak current (T_{90}) at –60 mV revealed a significant decrease by >20 s with DAMGO + CCh (Fig. 1*E*). The fast current development was also seen in cells that co-expressed $G_{i/o}$-coupled M2R and TRPC4β, which allowed simultaneous $G_{q/11}$ and $G_{i/o}$ stimulation by CCh (Fig. 1*E*) or an exposure to epidermal growth factor (EGF) to activate PLCγ before DAMGO application (*SI Appendix*, Fig. S5 *D–F*). Thus, coincident PLC stimulation enhances not only the probability but also kinetics of $G_{i/o}$ activation of TRPC4.

Dual Effects of PIP_2. Although a physical interaction between $G\alpha_{i/o}$ and TRPC4 C terminus has been suggested to underlie the mechanism of $G_{i/o}$ action (3), how PLC affects TRPC4 gating remains mysterious. PLC activation causes a breakdown of PIP_2, generation of diacylglycerols (DAGs) and inositol 1,4,5-trisphosphate (IP_3), which activates IP_3 receptors (IP_3Rs) to mobilize Ca^{2+} from the endoplasmic reticulum (17). DAGs activate TRPC3/C6/C7 but not TRPC4/C5 (18, 19). IP_3Rs were shown to facilitate activation of all TRPCs by competing with Ca^{2+}–calmodulin for binding to the conserved C-terminal calmodulin and IP_3R-binding (CIRB) site (20–23). Incidentally, the CIRB site is also critical for the $G\alpha_{i/o}$ effect on TRPC4 (3). Moreover, Ca^{2+} exhibits both positive and negative effects on some TRPC channels (20, 24–28).

To define the critical PLC signaling components for TRPC4 activation, we first examined PIP_2. Previously, PIP_2 was shown to inhibit activation of TRPC4α (2) but prevent desensitization of TRPC4β (29). Using zebrafish voltage-sensitive phosphatase (DrVSP) to reduce PIP_2 content by dephosphorylation without a concomitant breakdown to DAG and IP_3 (30), we observed a marked depression of the TRPC4β current evoked by either DAMGO or DAMGO + CCh upon phosphatase activation by a brief depolarization pulse (100 mV, 0.5 s) (Fig. 2 *A* and *B*). This suggests that either PIP_2 itself or one of its breakdown products is needed to support TRPC4β activity.

Noticeably, repeated DrVSP activation abolished the slow phase of the biphasic response to DAMGO (Fig. 2*A*). T_{90} was shortened but did not reach statistical significance ($P = 0.1$); however, T_{50} was significantly shorter with DrVSP (Fig. 2*C*), suggesting an acceleration of the initial phase and a likely slowdown of the second rapid rising phase. We reasoned that this could indicate a tonic inhibition by the resting level of PIP_2. To test this possibility, we lowered DAMGO to 30 nM, which evoked only a very weak current in control cells. However, in DrVSP-expressing cells subjected to depolarization pulses, 30 nM DAMGO induced a sizable TRPC4β current (Fig. 2 *D* and *E*). Similarly, dephosphorylating PIP_2 with rapamycin-induced membrane translocation of yeast inositol polyphosphate 5-phosphatase, Inp54p (31), also facilitated TRPC4β activation by weak μOR stimulation (*SI Appendix*, Fig. S6). Therefore, in addition to supporting TRPC4 function, PIP_2 also exerts a tonic inhibition on the channel.

Ca^{2+} Improves the Probability but Not the Rate of $G_{i/o}$-Mediated TRPC4 Activation. Downstream from the PIP_2 breakdown, IP_3R activation and $[Ca^{2+}]_i$ rise have been reported to support TRPC4/C5 function (21, 24–28, 32). To determine if IP_3Rs are involved in TRPC4 activation, we applied the IP_3R inhibitor heparin (3 mg/mL) by intracellular dialysis and found that most cells failed to respond to DAMGO and subsequent application of CCh (Fig. 3 *A–C*). However, addition of a Ca^{2+} ionophore, ionomycin (IM, 10 μM), rescued the response (Fig. 3 *B* and *C*). IM causes a $[Ca^{2+}]_i$ rise without activating IP_3Rs, suggesting that IP_3R-mediated endoplasmic reticulum Ca^{2+} release is a key event in PLC signaling to induce TRPC4β activation.

A small number of heparin-treated cells (3 out of 10, marked in red in Fig. 3*C*) responded to DAMGO, with peak current density comparable to controls. This could arise from either an incomplete block of IP_3Rs or an IP_3R-independent $[Ca^{2+}]_i$ rise. Presumably, a triggering $[Ca^{2+}]_i$ rise provided by IP_3Rs or other means could open a few TRPC4β channels, which would be followed by opening more channels in the cell through a positive-feedback mechanism due to Ca^{2+} influx via these channels. Supporting the very strong cytosolic Ca^{2+} dependence, DAMGO-evoked TRPC4β activation was strongly influenced by Ca^{2+} buffering strength of the pipette solution,

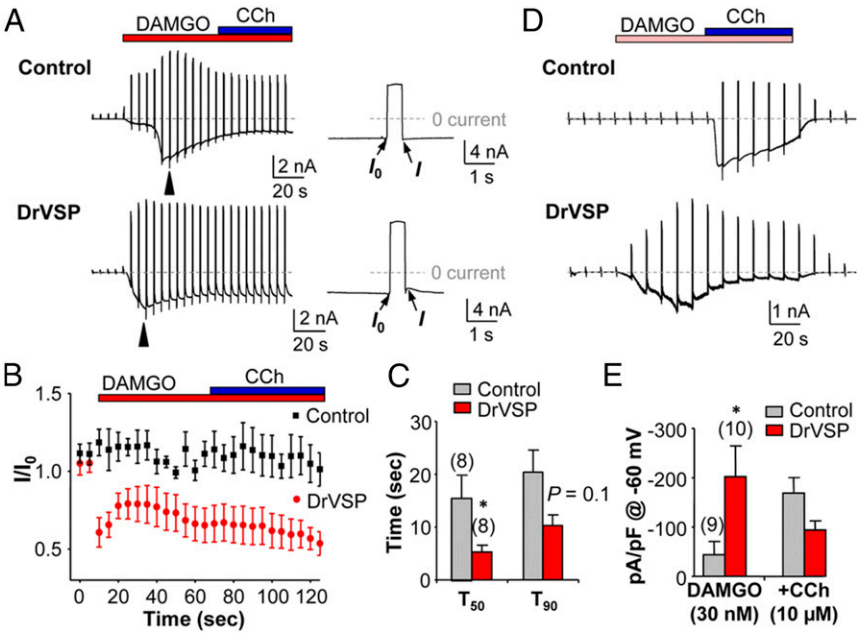

Fig. 2. Dual effects of PIP_2 on $G_{i/o}$-mediated TRPC4 activation. μOR/C4β cells were transiently transfected with either a control vector or cDNA encoding DrVSP. The pipette solution had 0.05 mM EGTA and no Ca^{2+}. (*A*) Cells were held at –60 mV, whereas depolarization pulses (100 mV, 0.5 s) were applied every 5 s. DAMGO (1 μM) and CCh (10 μM) were applied as indicated. Note the decrease in current amplitude immediately following each pulse in the DrVSP-transfected cell. Sections pointed by the arrowheads are expanded on right with I_0 (current before pulse) and I (current after pulse) indicated. (*B*) Time courses of I/I_o for control and DrVSP cells (means ± SEM, $n = 6$ for each). No current depression was detected in control cells or before DAMGO in DrVSP cells. (*C*) Summary of T_{50} and T_{90} by DAMGO. Although T_{90} did not reach statistical significance, T_{50} values are different. The near doubling of T_{90} versus T_{50} in DrVSP cells indicates monophasic current development. (*D*) Subthreshold DAMGO (30 nM) activated TRPC4β currents in DrVSP but not control cells. Depolarization pulses were applied at 10-s intervals. (*E*) Summary of peak current density at –60 mV for experiments illustrated in *D*. $^*P < 0.05$ versus controls by *t* test.

with ≤0.05 mM EGTA allowing current development in 100% cells, 0.5 mM EGTA supporting that in <50% cells, and 5 mM EGTA completely inhibiting the current (*SI Appendix*, Fig. S5 *A* and *B*). Also, DAMGO evoked very small currents when Ca^{2+} was removed from the bath solution (*SI Appendix*, Fig. S7*A*), indicating that continued Ca^{2+} influx is needed to support TRPC4 currents.

With 0.2–0.5 mM EGTA in the pipette solution, TRPC4β activation by DAMGO was suboptimal. However, those cells that failed to respond to DAMGO (Grp II) responded to subsequent addition of not only CCh (Fig. 1 *B* and *D*) but also IM (Fig. 3 *D* and *F*). By contrast, neither IM alone nor IM + CCh induced a discernible TRPC4β current, whereas subsequent application of DAMGO to these cells gave robust currents (Fig. 3 *E* and *F* and *SI Appendix*, Fig. S7*B*). Interestingly, in the absence of external Ca^{2+}, IM only weakly facilitated $G_{i/o}$ activation of TRPC4 (*SI Appendix*, Fig. S7 *C–E*), indicating that Ca^{2+} influx strongly impacts the current development in the presence of IM. Moreover, currents induced by DAMGO + IM still exhibited biphasic kinetics, with T_{90} significantly longer than when CCh was included (Fig. 3*G*), suggesting that IM treatment, or $[Ca^{2+}]_i$ rise, did not completely reproduce the effect of $G_{q/11}$–PLCβ stimulation on TRPC4 activation.

To determine the $[Ca^{2+}]_i$ needed to activate TRPC4, we clamped free Ca^{2+} levels in pipette solutions by 10 mM BAPTA [1,2-bis(o-aminophenoxy)ethane-N,N,N′,N′-tetraacetic acid], minimizing Ca^{2+} fluctuations during whole-cell recordings. With free $[Ca^{2+}]_i$ clamped to 100 nM, neither DAMGO alone nor DAMGO + CCh evoked TRPC4 currents (*SI Appendix*, Fig. S8*A*). Increasing $[Ca^{2+}]_i$ to >1 μM allowed DAMGO to induce currents, which reached the maximum at ∼10 μM $[Ca^{2+}]_i$ (*SI Appendix*, Fig. S8 *A* and *B*). Then, the currents became smaller at ≥50 μM free $[Ca^{2+}]_i$, indicating a dual dependence on $[Ca^{2+}]_i$ (*SI Appendix*, Fig. S8*B*). Fitting the Ca^{2+}-dependent changes of TRPC4 currents with a biphasic Hill equation (33) yielded an EC_{50} of ∼12 μM and an IC_{50} of ∼28 μM for Ca^{2+}-dependent facilitation and inhibition, respectively, suggesting a very narrow $[Ca^{2+}]_i$ range for TRPC4 activation. With $[Ca^{2+}]_i$ clamped at 10 μM, the extracellular Ca^{2+} dependence was markedly reduced (*SI Appendix*, Fig. S8*E*). Altogether, the above results demonstrate the importance of $[Ca^{2+}]_i$ rise in $G_{i/o}$-mediated TRPC4 activation; however, Ca^{2+} alone was insufficient to recapitulate the facilitation by PLC on activation kinetics.

PLCδ1 Is Involved in TRPC4 Activation. Testing other components of the PLC pathway, we found no evidence for involvement of IP_3, DAG, or PKC in $G_{i/o}$ activation of TRPC4 even with $[Ca^{2+}]_i$ raised by IM (*SI Appendix*, Fig. S9 *A–C*). Interestingly, the presence of TRPC4β strongly enhanced agonist-evoked PLC activity (*SI Appendix*, Fig. S9*D*). It is likely that Ca^{2+} influx through TRPC4 also enhances PLC function, as most PLC isoforms are Ca^{2+} sensitive and some are directly activated by Ca^{2+}—for example, PLCδ (34).

To test whether a specific PLC isozyme is involved in TRPC4 activation, we knocked down PLC isoforms typically associated with $G_{q/11}$ and Ca^{2+} signaling in HEK293 cells (35) by siRNA. Intriguingly, knockdown of PLCδ1 but not PLCδ3, PLCβ1, or PLCβ3 inhibited TRPC4 activation (*SI Appendix*, Fig. S10). Furthermore, expression of either the Ca^{2+}-insensitive, dominant-negative PLCδ1 mutant E341R/D343R (δ1-DN) (36) (but not the analogous PLCδ3 mutant E382R/D384R, δ3-DN) or the lipase-deficient PLCδ1 mutant H311A (37) strongly inhibited TRPC4β regardless of whether CCh was co-applied with DAMGO (Fig. 4 *A* and *B*). δ1-DN also inhibited TRPC4α but not TRPC5 (*SI Appendix*, Fig. S11*A*), and it completely abolished the facilitation of DAMGO activation of TRPC4β by EGF (*SI Appendix*, Fig. S11 *C* and *D*). Conversely, overexpression of wild-type PLCδ1 or PLCδ3 (but not PLCβ1/β2) significantly reduced T_{90} of the DAMGO-evoked TRPC4β current without affecting peak amplitude (Fig. 4 *A–C*). However, only PLCδ1, but not the other PLC isozymes, significantly rescued the inhibition by δ1-DN (*SI Appendix*, Fig. S11*B*). Thus, PLCδ1 is not only necessary but also rate limiting for TRPC4 activation.

PLCδ1 is inhibited by RhoA (36, 38). Indeed, expression of a constitutively active RhoA mutant (L63) strongly inhibited TRPC4β (*SI Appendix*, Fig. S12 *A* and *B*). By contrast, expression of a DN RhoA mutant (N19) or RhoA-suppressing C3 exoenzyme accelerated the rate of TRPC4β activation without affecting peak amplitude (*SI Appendix*, Fig. S12 *A–C*), suggesting that RhoA inhibition of PLCδ1 might underlie the slow kinetics of $G_{i/o}$-mediated TRPC4 activation. Importantly, inhibition by RhoA-L63 was reversed by co-expression of a constitutively active PLCδ1 mutant (δ1-ΔXY) (39) (*SI Appendix*, Fig. S12 *A* and *B*). As controls, we verified that the PLCδ1 and RhoA mutants affected neither CCh-stimulated Ca^{2+} store release nor TRPC4β surface expression (*SI Appendix*, Fig. S12 *D–F*), indicating that the $G_{q/11}$–PLCβ pathway and TRPC4β trafficking remained intact under these conditions.

PLCδ1 Is Critical for $G_{i/o}$ Activation of Endogenous TRPC4-Containing Channels. Recently, TRPC4 was shown to be expressed in renal cancer cells A-498 and directly activated by englerin A (6, 7). We found that similar currents were elicited by adenosine (1–100 μM), which were blocked by PTX and a TRPC4/C5 antagonist, M84 (40)

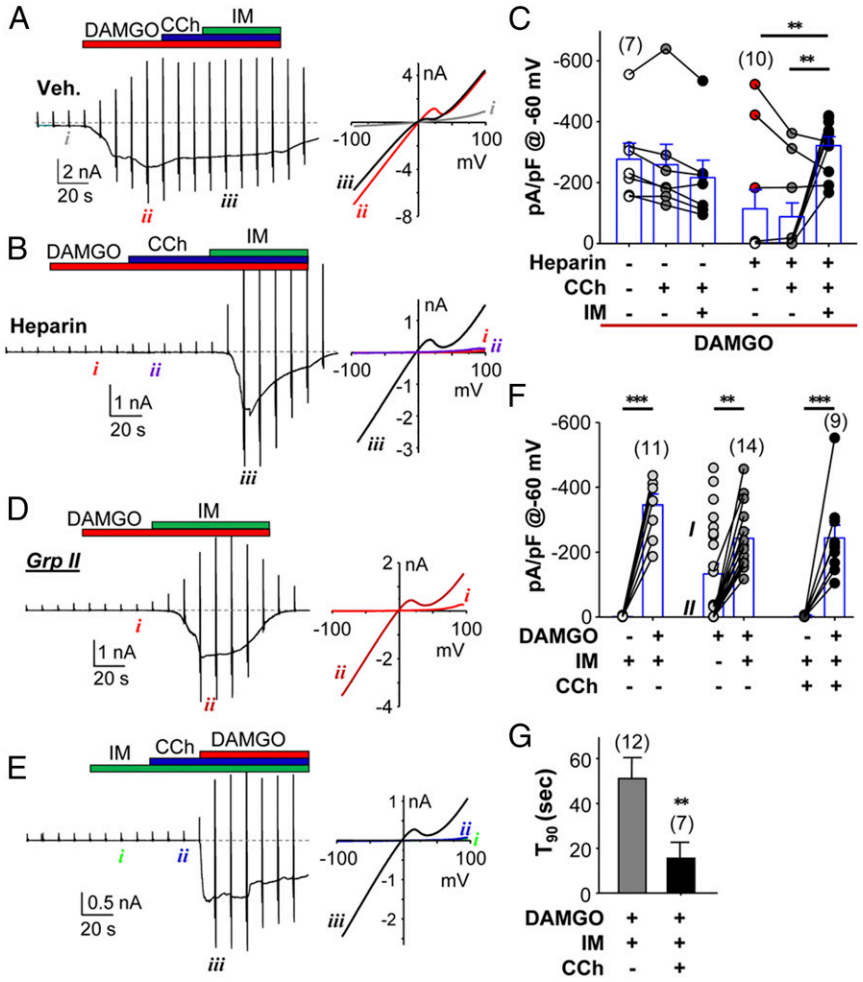

Fig. 3. Intracellular Ca^{2+} improves the probability but not the rate of $G_{i/o}$-mediated TRPC4 activation. μOR/C4β cells were used. (*A*–*C*) Heparin suppressed TRPC4 activation by DAMGO ± CCh. Vehicle (Veh, *A*) or heparin (3 mg/mL, *B*) was infused into cells by pipette dialysis for >5 min before DAMGO (1 μM), CCh (10 μM), and IM (10 μM) were applied extracellularly. Whole-cell currents and I–V curves show a lack of or very weak response to DAMGO and DAMGO + CCh in a heparin-treated cell. IM rescued the response (*B*). (*C*) Peak current density at –60 mV induced by DAMGO ± CCh or IM for individual cells treated or not by heparin. Blue boxes and bars show means ± SEM. (*D*–*F*) Facilitation of TRPC4 activation by IM. DAMGO-irresponsive cells (Grp II) became activated in the presence of IM (*D*), but IM ± CCh failed to elicit a current until DAMGO was introduced (*E*). (*F*) Peak current density at –60 mV induced by DAMGO, CCh, and IM. Only Grp II cells were further treated with IM. (*G*) T_{90} for currents evoked by DAMGO + IM ± CCh. The pipette solution contained 0.2 mM EGTA and no Ca^{2+}. $^{**}P \leq 0.01$, $^{***}P \leq 0.001$ by ANOVA for *C*; *t* test for *F* and *G*.

(*SI Appendix*, Fig. S13 *C*–*G*). The currents were sensitive to $[Ca^{2+}]_i$ buffering (*SI Appendix*, Fig. S14 *A* and *B*). However, unlike englerin A, adenosine-evoked activation was slow, exhibiting biphasic kinetics reminiscent of DAMGO activation of TRPC4β in HEK293 cells. Importantly, the adenosine-evoked current was significantly reduced by siRNA against PLCδ1 but not other PLC isoforms (*SI Appendix*, Fig. S14 *C* and *D*) and strongly suppressed by the expression of PLCδ1-DN or RhoA-L63 (Fig. 5 *A* and *B*). PLCδ1-ΔXY rescued the adenosine-evoked current in RhoA-L63–expressing cells (Fig. 5 *A* and *B*). Both PLCδ1-ΔXY and RhoA-N19 accelerated the rate of current activation by adenosine (Fig. 5 *A* and *C*). Thus, PLCδ1 is also involved in the activation of endogenous TRPC4-containing channels in A-498 cells by $G_{i/o}$-coupled adenosine receptors. Incidentally, histamine elicited currents in A-498 cells with similar I–V relationship as the adenosine-evoked ones, but they were not inhibited by PTX or TRPC antagonists, indicative of a non-TRPC mechanism (*SI Appendix*, Fig. S13 *E*–*G*). Thus, although histamine elicited a robust $[Ca^{2+}]_i$ rise (*SI Appendix*, Fig. S13 *A* and *B*) and markedly enhanced both the rate and amplitude of currents when co-applied with adenosine (*SI Appendix*, Fig. S13 *G* and *H*), reminiscent of CCh in TRPC4/μOR-expressing HEK293 cells, these effects likely include $G_{q/11}$–PLCβ actions via both TRPC4-dependent and -independent mechanisms.

Discussion

Although TRPC channels are commonly thought of as receptor-operated channels gated by PLC signaling, we show here that the PLCβ or PLCγ pathway may not be essential for TRPC4 activation. Rather, the channel requires $G_{i/o}$ proteins for activation and exhibits an unexpected dependence on PLCδ1, making it a coincidence detector of $G_{i/o}$ and PLCδ1 signaling. PIP_2 is both a substrate and a membrane docking site, whereas Ca^{2+} is the main activator of PLCδ (34, 41). Therefore, PLCδ1 may be central for the PIP_2 and Ca^{2+} dependence of TRPC4 activation. Also, by inhibiting PLCδ1, the small GTPase RhoA likely contributes to the biphasic kinetics of the $G_{i/o}$-activated TRPC4 current. Whereas RhoA inhibition (by N19) accelerated, its persistent stimulation (by L63) suppressed channel activation. The latter was reversed by the constitutively active mutant of PLCδ1, supporting that RhoA acts via PLCδ1 on TRPC4 activation.

Intriguingly, inhibiting PLCδ1 abolished the effect of not only $G_{i/o}$ but also $G_{i/o}$ and $G_{q/11}$ (or EGF) co-stimulation, implicating a unique role of PLCδ1 that cannot be substituted by other PLC isoforms. An exception may be the closely related PLCδ3, which enhanced the rate of DAMGO activation of TRPC4β but failed to rescue the inhibition by PLCδ1-DN. The failure of PLCδ3 siRNA and the DN mutant to inhibit TRPC4 also suggests that PLCδ3 plays a lesser role than PLCδ1 on TRPC4 activation, which may be accounted for by the difference in either expression or coupling efficiency. Alternatively, the kinetic effect of PLCδ3 overexpression may be explained by its role in down-regulating RhoA (42).

The strict requirement on PLCδ1 indicates an intimate coupling and/or possibly a physical interaction between PLCδ1 and TRPC4. The lack of effect of PLCδ1 inhibition on TRPC5 activation further argues for the coupling specificity. However, our repeated attempts did not yield evidence of physical association between PLCδ1 and TRPC4 (*SI Appendix*, Fig. S15), suggesting that they do not exist in the same complex, which perhaps explains the high sensitivity of this coupling to Ca^{2+} buffering. Nevertheless, we show a similar dependence on Ca^{2+} and PLCδ1 of $G_{i/o}$-mediated activation of

endogenous TRPC4-containing currents via adenosine receptors in renal cancer A-498 cells. The currents exhibited outward rectification typical of TRPC1/C4 heteromers (43) and similar to that activated by the TRPC4/C5 agonist englerin A (6, 7). Interestingly, the englerin A-evoked currents were independent of PLCδ1 (*SI Appendix*, Fig. S16), indicating that the PLCδ1 dependence is uniquely coupled to $G_{i/o}$ activation of TRPC4-containing channels, both native and heterologously expressed.

PIP_2 exerts both positive and negative effects on TRPC channels (2, 29, 44, 45), but the mechanisms remain mysterious. The DAG-sensitive TRPC3/C6/C7 channels seemed to require both PIP_2 itself and its product, DAG, to maintain channel activity (46, 47). Although TRPC4/C5 are not sensitive to DAG, increasing PIP_2 levels also helped sustain the activation of TRPC4β and C5 (29, 48). For TRPC4, the PIP_2 dependence may be explained by the fact that membrane translocation of PLCδ1 requires this lipid (41), but this will not be applicable to TRPC5, which is not dependent on PLCδ1. To inhibit TRPC, PIP_2 may physically bind to TRPC4 in the C-terminal region present in the α but missing in the β isoform (2) or interact with TRPC4/C5 in a Ca^{2+}-dependent manner through SESTD1, a protein that binds to the CIRB site (49). We show here that dephosphorylating PIP_2 facilitated TRPC4β activation during weak $G_{i/o}$ stimulation. This differs from the previous study showing that exogenously added PIP_2 specifically inhibited TRPC4α, but not C4β, when $G_{i/o}$ and $G_{q/11}$ pathways were co-stimulated (2). Together, these data suggest two forms of tonic PIP_2 inhibition on TRPC4—one unique to TRPC4α and another common to both—as TRPC4α incorporates the entire sequence of C4β (23). Because the latter is only obvious with weak $G_{i/o}$ and no $G_{q/11}$–PLCβ stimulation, its affinity to PIP_2 must be very low. Thus, reducing $[PIP_2]$ is one of the actions by which PLC facilitates TRPC4 activation.

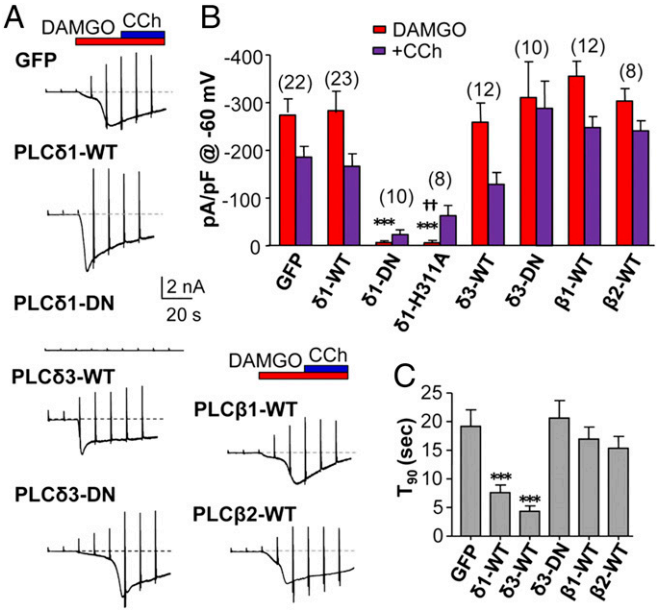

Fig. 4. PLCδ1 is necessary for DAMGO-evoked TRPC4 activation. μOR/C4β cells were transiently transfected with either a control vector (GFP) or cDNA encoding various PLC constructs as shown. The pipette solution contained 0.05 mM EGTA and no Ca^{2+}. (*A*) Representative whole-cell currents in response to DAMGO (1 μM) and CCh (10 μM). DN, dominant-negative, E341R/D343R for PLCδ1 and E382R/D384R for PLCδ3; WT, wild type. Note the lack of current with PLCδ1-DN and the faster rate of DAMGO-evoked current with PLCδ1-WT and PLCδ3-WT compared with PLCβ1/β2. (*B*) Summary of peak current density at –60 mV evoked by DAMGO ± CCh. (*C*) T_{90} for DAMGO-evoked current at –60 mV. ***$P < 0.001$ for δ1-DN versus GFP/δ1-WT/δ3-WT/δ3-DN/β1-WT/β2-WT and δ1-H311A versus GFP/δ1-WT/δ3-WT/β1-WT in *B* and δ1-WT/δ3-WT versus GFP in *C*; ††$P < 0.01$ for δ1-H311A versus δ3-DN/β2-WT in *B* by ANOVA.

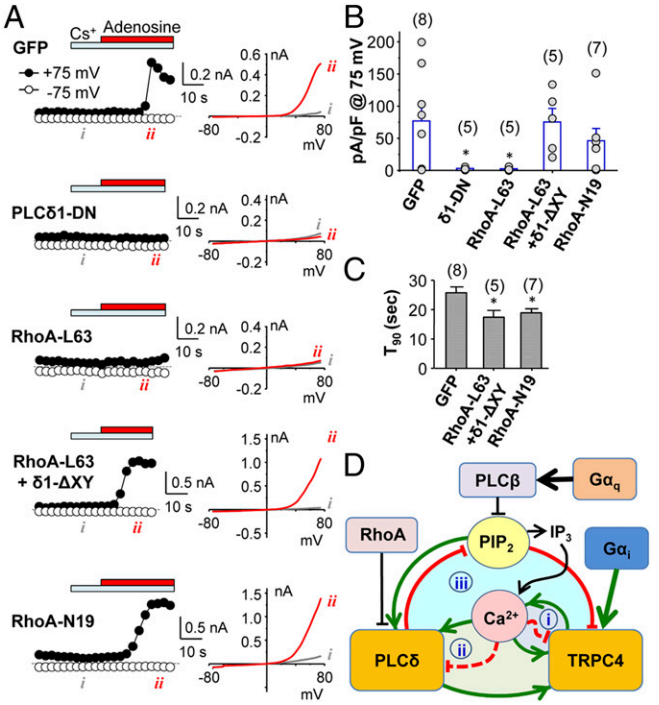

Fig. 5. PLCδ1 is necessary for $G_{i/o}$ activation of endogenous TRPC4-like currents in A-498 cells. (*A–C*) A-498 cells were transiently transfected with GFP (control) or PLCδ1 and RhoA mutants as shown. The pipette solution contained no EGTA or Ca^{2+}. Whole-cell currents were recorded by voltage ramps from +100 to –100 mV (see *SI Appendix*, Fig. S13*C*) at 1 Hz. Na^+ in the bath was replaced by Cs^+ to facilitate current activation by adenosine (1 μM). (*A*) Representative time courses of currents at –75 and +75 mV (*Left*) and I–V curves (Right) at the indicated time points. (*B*) Peak current density at +75 mV evoked by adenosine for individual cells and means ± SEM (blue boxes and bars). (*C*) T_{90} for adenosine-evoked currents at +75 mV. *$P < 0.05$ versus GFP by *t* test. (*D*) Diagram of PLCδ1–TRPC4 self-reinforcing system. Positive and negative effects necessary for TRPC4 activation are indicated in green and red lines, respectively. Nonessential, modulatory effects are indicated in black. In addition to activating PLCδ1, Ca^{2+} might directly enhance channel function, based on previous work with TRPC5 and native channels containing TRPC4. Thus, at least three self-reinforcing loops exist to sustain TRPC4 activity when $G_{i/o}$ is active: positive feedback effects between Ca^{2+} and TRPC4 (*i*); among PLCδ1, Ca^{2+} and TRPC4 (*ii*); as well as a double-negative effect among PLCδ1, PIP_2, and TRPC4, which is continuously supported by Ca^{2+} that links TRPC4 function to PLCδ1 activation (*iii*). The system is facilitated by the $G_{q/11}$–PLCβ pathway, which provides the Ca^{2+} signal for PLCδ1 activation and helps lower the barrier of channel gating by reducing PIP_2. It is negatively regulated by RhoA (through inhibiting PLCδ1) and high Ca^{2+} levels, which may inhibit either TRPC4 or PLCδ1, or both (dashed lines).

Ca^{2+} appears to be a downstream factor from PIP_2 hydrolysis that supports TRPC4 activation. Because Ca^{2+} influx through open TRPC4 channels also provides continued $[Ca^{2+}]_i$ rise, the reliance on PIP_2 to produce a Ca^{2+} signal could be extraneous except for generating an initial trigger. As micromolar $[Ca^{2+}]_i$ is needed for TRPC4 activation and the channel is also inhibited by slightly higher $[Ca^{2+}]_i$, the dynamics of $[Ca^{2+}]_i$ change must be critical. With low [EGTA] that allows $[Ca^{2+}]_i$ to fluctuate, peak currents were about twofold higher than when $[Ca^{2+}]_i$ was clamped to 10 μM by BAPTA, supporting the importance of spatiotemporal dynamics of Ca^{2+} in TRPC4 regulation. However, Ca^{2+} alone did not recapitulate the effect of CCh on activation kinetics, suggesting involvement of additional components of PLC signaling in TRPC4 gating. We did not find any effect of IP_3, DAG, and PKC on either amplitude or kinetics of IM + DAMGO-evoked TRPC4β currents or when channel activation was suppressed by PLCδ1-DN (*SI Appendix*, Fig. S11*E*). Rather, our data suggest that the rate-limiting step is PLCδ1 (and possibly also PLCδ3) activation, on which both Ca^{2+} and PIP_2 may converge to control channel gating. PIP_2 hydrolysis and Ca^{2+} signals

generated from PLCδ1 activity could further enhance channel opening. Altogether, the PLCδ1–TRPC4 duet forms a self-reinforcing loop for continued channel activation in a Ca^{2+}- and PIP_2-dependent fashion. The system requires $G_{i/o}$ activation, with $G_{q/11}$–PLCβ (or another PLC) acting as an accelerator and RhoA as a brake (Fig. 5*D*). Because of the dual regulation by both Ca^{2+} and PIP_2, the system should also be very sensitive to signaling processes that alter the levels of these intracellular messengers, making TRPC4 a versatile sensor and integrator of diverse transmitter inputs, critical for its functions in neurons and muscles.

Interestingly, persistent TRPC4 activation was observed in lateral septal neurons exposed very briefly to a metabotropic glutamate receptor agonist in a manner dependent on $[Ca^{2+}]_i$ changes and voltage-gated Ca^{2+} channel activation (12), adding another variable in native cells where membrane depolarization and Ca^{2+} entry via voltage-gated channels can be critical for TRPC4 function. Moreover, an interplay among $G_{i/o}$, PLCδ1, and Ca^{2+} entry channels has been documented in rabbit gastric smooth muscle, where activation of $G_{i/o}$-coupled receptors caused delayed activation of PLCδ1 in a manner thought to depend on store-operated Ca^{2+} entry and inhibited by RhoA (36). However, the pharmacology used and the presence of TRPC4 in these cells (50) would argue that the entry channel was formed by TRPC4. Therefore, not only does PLCδ1 support TRPC4 activation, but TRPC4 function also enhances PLCδ1 activity (see also *SI Appendix*, Fig. S9*D*). The positive feedback loops formed by this system should have strong implications to its function as an environmental and stress sensor in various cell types.

Methods

Cell lines, cell culture, and transfection were as previously described (2, 13). Details on cell culture, drug treatment, electrophysiological protocols and solutions, fluorescence imaging, surface biotinylation, Western blotting, and data analysis are explained in the figure legends and *SI Appendix, SI Methods*.

ACKNOWLEDGMENTS. We thank Drs. J. Frost, T. Meyer, Y. Okamura, and J. Sondek for cDNA constructs; B. Fang for A-498 cells; and G. Du for transfection reagent. This work was supported in part by NIH Grants DK081654 and NS092377 (to M.X.Z.) and Sonderforschungsbereich/Transregio 152 (to V.F.). D.P.T. is a recipient of a predoctoral fellowship of the American Heart Association.

1. Venkatachalam K, Montell C (2007) TRP channels. *Annu Rev Biochem* 76:387–417.
2. Otsuguro K, et al. (2008) Isoform-specific inhibition of TRPC4 channel by phosphatidylinositol 4,5-bisphosphate. *J Biol Chem* 283(15):10026–10036.
3. Jeon JP, et al. (2012) Selective Gαi subunits as novel direct activators of transient receptor potential canonical (TRPC)4 and TRPC5 channels. *J Biol Chem* 287(21):17029–17039.
4. Kim J, et al. (2014) Isoform- and receptor-specific channel property of canonical transient receptor potential (TRPC)1/4 channels. *Pflugers Arch* 466(3):491–504.
5. Tiruppathi C, et al. (2002) Impairment of store-operated Ca^{2+} entry in $TRPC4^{(-/-)}$ mice interferes with increase in lung microvascular permeability. *Circ Res* 91(1):70–76.
6. Akbulut Y, et al. (2015) (-)-Englerin A is a potent and selective activator of TRPC4 and TRPC5 calcium channels. *Angew Chem Int Ed Engl* 54(12):3787–3791.
7. Carson C, et al. (2015) Englerin A agonizes the TRPC4/C5 cation channels to inhibit tumor cell line proliferation. *PLoS One* 10(6):e0127498.
8. Munsch T, Freichel M, Flockerzi V, Pape HC (2003) Contribution of transient receptor potential channels to the control of GABA release from dendrites. *Proc Natl Acad Sci USA* 100(26):16065–16070.
9. Tsvilovskyy VV, et al. (2009) Deletion of TRPC4 and TRPC6 in mice impairs smooth muscle contraction and intestinal motility in vivo. *Gastroenterology* 137(4):1415–1424.
10. Weick JP, Austin Johnson M, Zhang SC (2009) Developmental regulation of human embryonic stem cell-derived neurons by calcium entry via transient receptor potential channels. *Stem Cells* 27(12):2906–2916.
11. Phelan KD, et al. (2012) Heteromeric canonical transient receptor potential 1 and 4 channels play a critical role in epileptiform burst firing and seizure-induced neurodegeneration. *Mol Pharmacol* 81(3):384–392.
12. Tian J, et al. (2014) Dual depolarization responses generated within the same lateral septal neurons by TRPC4-containing channels. *Pflugers Arch* 466(7):1301–1316.
13. Miller M, et al. (2011) Identification of ML204, a novel potent antagonist that selectively modulates native TRPC4/C5 ion channels. *J Biol Chem* 286(38):33436–33446.
14. Plant TD, Schaefer M (2005) Receptor-operated cation channels formed by TRPC4 and TRPC5. *Naunyn Schmiedebergs Arch Pharmacol* 371(4):266–276.
15. Obukhov AG, Nowycky MC (2004) TRPC5 activation kinetics are modulated by the scaffolding protein ezrin/radixin/moesin-binding phosphoprotein-50 (EBP50). *J Cell Physiol* 201(2):227–235.
16. Kim H, et al. (2012) The roles of G proteins in the activation of TRPC4 and TRPC5 transient receptor potential channels. *Channels (Austin)* 6(5):333–343.
17. Berridge MJ, Lipp P, Bootman MD (2000) Signal transduction. The calcium entry pas de deux. *Science* 287(5458):1604–1605.
18. Hofmann T, et al. (1999) Direct activation of human TRPC6 and TRPC3 channels by diacylglycerol. *Nature* 397(6716):259–263.
19. Okada T, et al. (1999) Molecular and functional characterization of a novel mouse transient receptor potential protein homologue TRP7. Ca(2+)-permeable cation channel that is constitutively activated and enhanced by stimulation of G protein-coupled receptor. *J Biol Chem* 274(39):27359–27370.
20. Zhang Z, et al. (2001) Activation of Trp3 by inositol 1,4,5-trisphosphate receptors through displacement of inhibitory calmodulin from a common binding domain. *Proc Natl Acad Sci USA* 98(6):3168–3173.
21. Tang J, et al. (2001) Identification of common binding sites for calmodulin and inositol 1,4,5-trisphosphate receptors on the carboxyl termini of trp channels. *J Biol Chem* 276(24):21303–21310.
22. Vaca L, Sampieri A (2002) Calmodulin modulates the delay period between release of calcium from internal stores and activation of calcium influx via endogenous TRP1 channels. *J Biol Chem* 277(44):42178–42187.
23. Zhu MX (2005) Multiple roles of calmodulin and other Ca(2+)-binding proteins in the functional regulation of TRP channels. *Pflugers Arch* 451(1):105–115.
24. Kinoshita-Kawada M, et al. (2005) Inhibition of TRPC5 channels by Ca^{2+}-binding protein 1 in *Xenopus* oocytes. *Pflugers Arch* 450(5):345–354.
25. Ordaz B, et al. (2005) Calmodulin and calcium interplay in the modulation of TRPC5 channel activity. Identification of a novel C-terminal domain for calcium/calmodulin-mediated facilitation. *J Biol Chem* 280(35):30788–30796.
26. Gross SA, et al. (2009) TRPC5 is a Ca^{2+}-activated channel functionally coupled to Ca^{2+}-selective ion channels. *J Biol Chem* 284(49):34423–34432.
27. Blair NT, Kaczmarek JS, Clapham DE (2009) Intracellular calcium strongly potentiates agonist-activated TRPC5 channels. *J Gen Physiol* 133(5):525–546.
28. Shi J, et al. (2004) Multiple regulation by calcium of murine homologues of transient receptor potential proteins TRPC6 and TRPC7 expressed in HEK293 cells. *J Physiol* 561(Pt 2):415–432.
29. Kim H, et al. (2013) An essential role of $PI(4,5)P_2$ for maintaining the activity of the transient receptor potential canonical (TRPC)4β. *Pflugers Arch* 465(7):1011–1021.
30. Hossain MI, et al. (2008) Enzyme domain affects the movement of the voltage sensor in ascidian and zebrafish voltage-sensing phosphatases. *J Biol Chem* 283(26):18248–18259.
31. Suh BC, Inoue T, Meyer T, Hille B (2006) Rapid chemically induced changes of $PtdIns(4,5)P_2$ gate KCNQ ion channels. *Science* 314(5804):1454–1457.
32. Kanki H, et al. (2001) Activation of inositol 1,4,5-trisphosphate receptor is essential for the opening of mouse TRP5 channels. *Mol Pharmacol* 60(5):989–998.
33. Foskett JK, White C, Cheung KH, Mak DO (2007) Inositol trisphosphate receptor Ca^{2+} release channels. *Physiol Rev* 87(2):593–658.
34. Suh PG, et al. (2008) Multiple roles of phosphoinositide-specific phospholipase C isozymes. *BMB Rep* 41(6):415–434.
35. Atwood BK, Lopez J, Wager-Miller J, Mackie K, Straiker A (2011) Expression of G protein-coupled receptors and related proteins in HEK293, AtT20, BV2, and N18 cell lines as revealed by microarray analysis. *BMC Genomics* 12:14.
36. Murthy KS, Zhou H, Huang J, Pentyala SN (2004) Activation of PLC-δ1 by $G_{i/o}$-coupled receptor agonists. *Am J Physiol Cell Physiol* 287(6):C1679–C1687.
37. Ellis MV, U S, Katan M (1995) Mutations within a highly conserved sequence present in the X region of phosphoinositide-specific phospholipase C-delta 1. *Biochem J* 307(Pt 1):69–75.
38. Hodson EA, Ashley CC, Hughes AD, Lymn JS (1998) Regulation of phospholipase C-δ by GTP-binding proteins-rhoA as an inhibitory modulator. *Biochim Biophys Acta* 1403(1):97–101.
39. Hicks SN, et al. (2008) General and versatile autoinhibition of PLC isozymes. *Mol Cell* 31(3):383–394.
40. Zhu Y, et al. (2015) Identification and optimization of 2-aminobenzimidazole derivatives as novel inhibitors of TRPC4 and TRPC5 channels. *Br J Pharmacol* 172(14):3495–3509.
41. Allen V, Swigart P, Cheung R, Cockcroft S, Katan M (1997) Regulation of inositol lipid-specific phospholipase cdelta by changes in Ca^{2+} ion concentrations. *Biochem J* 327(Pt 2):545–552.
42. Kouchi Z, et al. (2011) Phospholipase Cdelta3 regulates RhoA/Rho kinase signaling and neurite outgrowth. *J Biol Chem* 286(10):8459–8471.
43. Strübing C, Krapivinsky G, Krapivinsky L, Clapham DE (2001) TRPC1 and TRPC5 form a novel cation channel in mammalian brain. *Neuron* 29(3):645–655.
44. Lemonnier L, Trebak M, Putney JW, Jr (2008) Complex regulation of the TRPC3, 6 and 7 channel subfamily by diacylglycerol and phosphatidylinositol-4,5-bisphosphate. *Cell Calcium* 43(5):506–514.
45. Trebak M, et al. (2009) Complex functions of phosphatidylinositol 4,5-bisphosphate in regulation of TRPC5 cation channels. *Pflugers Arch* 457(4):757–769.
46. Imai Y, Itsuki K, Okamura Y, Inoue R, Mori MX (2012) A self-limiting regulation of vasoconstrictor-activated TRPC3/C6/C7 channels coupled to $PI(4,5)P_2$-diacylglycerol signalling. *J Physiol* 590(Pt 5):1101–1119.
47. Itsuki K, et al. (2014) PLC-mediated $PI(4,5)P_2$ hydrolysis regulates activation and inactivation of TRPC6/7 channels. *J Gen Physiol* 143(2):183–201.
48. Kim BJ, Kim MT, Jeon JH, Kim SJ, So I (2008) Involvement of phosphatidylinositol 4,5-bisphosphate in the desensitization of canonical transient receptor potential 5. *Biol Pharm Bull* 31(9):1733–1738.
49. Miehe S, et al. (2010) The phospholipid-binding protein SESTD1 is a novel regulator of the transient receptor potential channels TRPC4 and TRPC5. *J Biol Chem* 285(16):12426–12434.
50. Lee KP, et al. (2005) TRPC4 is an essential component of the nonselective cation channel activated by muscarinic stimulation in mouse visceral smooth muscle cells. *Mol Cells* 20(3):435–441.